Adaptive Distortion Inversion Technique for LNA's Nonlinearity Compensation in Direct RF Digitization Receivers

Ngoc-Anh Vu[1], Hai-Nam Le[1], Thi-Hong-Tham Tran[2], Van-Phuc Hoang[1], Quang-Kien Trinh[1],
[1]Le Quy Don Technical University, 236 Hoang Quoc Viet Str., Hanoi, Vietnam
[2]Moscow Institute of Physics and Technology, Moscow, Russia
Email: ngocanh220484@gmail.com, namlh@mta.edu.vn

***Abstract*—This paper presents the analysis of the nonlinear distortion model of the Low Noise Amplifier (LNA) for multichannel direct RF digitization receivers (DRF–RX). The distortion model gives insights into the nature of the LNA distortions and is used as the fundamental ground for distortion compensation. The paper further presents a fully-digital solution using a reference channel accompanied by a least mean square (LMS) circuit for adaptive distortion compensation. The LMS circuit uses the information from the reference channel to invert the distortion impacts caused by the LNA's nonlinearity in the main channel and eventually recover the linear component.**

A direct RF digitization UHF receiver with 4-QPSK channels was implemented in Matlab to evaluate the proposed method's efficiency. The performance of the compensation circuits has been studied in detail. The simulation results show that the proposed solution greatly improves the receiver performance. Compared to the receiver without compensation, the compensation circuit helps to lower the distortion components by ~20 dB and improve the bit error rate (BER) by 2 orders of magnitude.

Keywords— Direct RF digitization, DCR, LNA distortion, digital receiver, LMS filter, distortion inversion, multichannel receiver, software-defined radio, UHF transceiver.

I. INTRODUCTION

Direct RF digitization receiver (DRF–RX) is one of the fully digital RF receiver architectures that has been widely applied in many commercial devices [1], [2] and currently draws considerable attention from the research community. DRF-RX architecture is a true Software-defined RXs, of which supports dynamic received band, multi-operation modes, and enables hardware reconfigurability. Furthermore, with the replacement of numerous analog components, the complexity and design cost of the DRF-RX are greatly reduced. More importantly, this architecture does not suffer from some permanent issues caused by those components in the conventional receivers such as I/Q imbalance distortions or DC offset component [3], [7]. However, when working in multichannel and wideband modes, DRF-RX still suffers from the distortions caused by LNA nonlinearity. This is an inevitable effect observed when the receiver simultaneously records multiple channels with different types of signal modulation and power levels [8]-[11]. In such a condition, when the total input power is high the LNA becomes saturated and partially works in the nonlinear region. Therefore, high energy channels after the LNA would end up generating nonlinear distortions. These distortions, in turn, degrade the signal quality of the nearby channels [8]–[11]. The effect of LNA nonlinearity is proportional to the power of the distortion channel, so it is a necessity to have a suitable and effective compensation method to tackle this issue.

In most of the prior arts, there are two basic solutions for distortion compensation; canceling or inverting all the nonlinear effects to obtain the useful signal. Accordingly, the fundamental task is to reproduce and/or to estimate the distortion components from the received signal. For example, estimation using band pass filters (BPF) was proposed in both solutions in [8, 11]. The method in [10] uses a variable high-frequency BPF to reproduce a part of distorted information and use it to evaluate the distortion. A solution using a linear reference receiver to reproduce and suppress distortion is proposed in [9]. However, these solutions have several technical limitations, e.g. variable high-frequency BPF [10] is not practical for implementation and/or the received band has to be known in advance [8, 11]. And the most important thing is that these techniques and the corresponding models are used for the common direct conversion receivers (DCRs) with the analog sub-circuit (i.e., quadrature mixers). Thus, the compensation circuit was highly complex due to the presence of many types of distortions.

In this work, we systematically studied the model of the LNA distortions and analyzed their impacts on DRF-RX. The LNA nonlinearity model is derived directly from the well-known Hammerstein's model [9]–[11]. Based on this model, we have developed an adaptive distortion compensation scheme for multichannel wideband specialized for DRF-RXs. Those interference components are then adaptively and "blindly" compensated from the total main channel's received signal. The complexity and the convergence speed of the LMS circuit are studied in detail. The effectiveness of the implemented circuits is evaluated by the spectral analysis and the BER performance.

The remaining of the paper is organized as follows. Section II presents distortion models of LNA and analyzes the effect of distortion on the multichannel DRF-RX model. Section III describes the LNA's nonlinearity compensation circuits using

the distortion inversion technique. Section IV presents the simulation results and the conclusions are drawn in section V.

II. Nonlinear LNA Distortions Models and Their Impacts on DRF-RXs

The generic structure of DRF-RX is shown in Fig. 1. An array of LPFs is still required to attenuate the out-of-band frequencies. Those LPFs do not have a strict requirement in selectivity as their main function is to lower the out-of-band frequencies energy, and they theoretically do not add any extra noise components. Then, the filtered signal is going through an LNA before being digitalized by a high-speed ADC. According to [13], [16], the state of the art ADCs have the resolutions of 14 bits, which corresponds to an approximate SFDR of 76 dB [13]. A gain factor of about 25 dB must be achieved to ensure the receiver sensitivity of less than -100 dBm [15]. Hence, the LNA is an indispensable component in any DRF-RX designs [3], [11]. Unfortunately, the LNAs only work linearly within a limited input power range. When the input signal energy exceeds the linear threshold, the amplifier becomes saturated and nonlinear distortions appear at the amplifier output [3]-[12]. The LNA nonlinear distortions consist of self-affected distortions caused by an individual RF signal to itself and distortions caused by the interference of other RF signals [3], [12]. According to Hammerstein's model [9]–[11], the RF signal, including nonlinear components, is assumed to be a polynomial with the form

$$y_{RF}(t) = \sum_{i=1}^{k} a_i(t) x_{RF}(t) \quad (1),$$

where $x_{RF}(t)$ and $y_{RF}(t)$ are LNA input and output respectively; $a_i(t)$ is the i[th]-order component coefficient. The input signal $x_{RF}(t)$, in turn, is represented as

$$x_{RF}(t) = 2Re[x(t)e^{j\omega_c t}] = x(t)e^{j\omega_c t} + x^* e^{-j\omega_c t} \quad (2),$$

where $x(t)$ is the baseband signal of $x_{RF}(t)$, $x(t)$ can be a single carrier frequency or multiple separate carrier frequencies; $\omega_c = 2\pi f_c$, with f_c is the center carrier frequency and (.)* represents the complex conjugate operation

The bandwidth of the DRF-RXs is typically large (a few tens to hundreds MHz). Therefore, the signal of a single channel can be distorted by harmonics and inter-modulation generated from far-away channels. The distortion models can be derived by applying the full distortion model as shown in (11). However, in practice, it is sufficient to consider up to the third-order distortions [14] and the RF nonlinear model can be simplified as

$$y_{RF}(t) = a_1 x_{RF}(t) + a_2 x_{RF}^2(t) + a_3 x_{RF}^3(t) \quad (3)$$

If the carrier frequency is large, the second-order component in (3) is located outside the received bandwidth and only the third component needs to be taken into consideration.

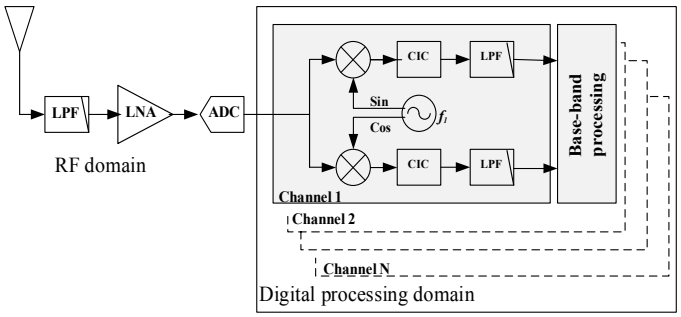

Fig. 1. The architecture of multichannel direct digitization receiver.

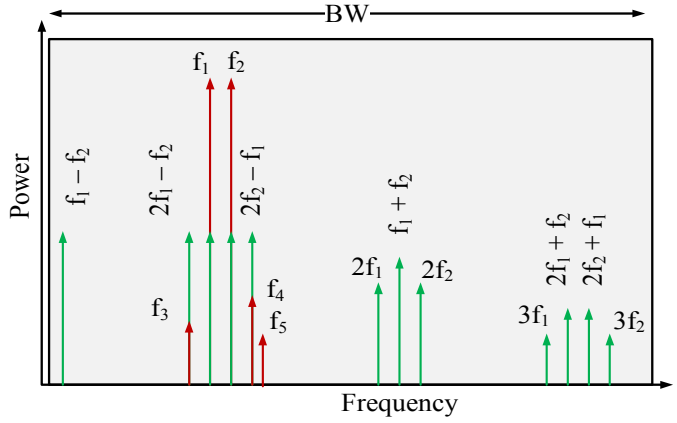

Fig. 2. The nonlinear components of LNA modeled with two-tone input.

However, with a low carrier frequency, this component is unignorable as the even and odd-order harmonics can still locate in the received bandwidth (see Fig. 3), which can be expressed as

$$x_{RF}^2(t) = 2A^2(t) + x^2(t)e^{2\omega_c t} + [x^*(t)]^2 e^{-j2\omega_c t} \quad (4),$$

where $2x(t)x^*(t) = 2A^2(t)$ is the spectrum around the DC component.

In (4), the even distorted components appear at zero and $\pm 2\omega_c$, but none appears at ω_c. This guarantees that the generated distortion does not affect itself and the adjacent but it does affect other channels around $2\omega_c$.

The third component in (3) in turn can be represented as

$$\begin{aligned} a_3 x_{RF}^3(t) &= a_3\{x(t)e^{j\omega_c t} + x^*(t)e^{-j\omega_c t}\}^3 \\ &= a_3\{x^3(t)e^{j3\omega_c t} + 3x^2(t)x^*(t)e^{j\omega_c t} \\ &\quad + 3x(t)[x^*(t)]^2 e^{-j\omega_c t} + [x^*(t)]^3 e^{-j3\omega_c t}\} \end{aligned} \quad (5)$$

As can be seen from (5), the distortion frequencies around ω_c, generated by component $3x^2(t)x^*(t)e^{j\omega_c t}$ affects itself and the adjacent channels while the component $x^3(t)e^{j3\omega_c t}$ affects channels around $3\omega_c$.

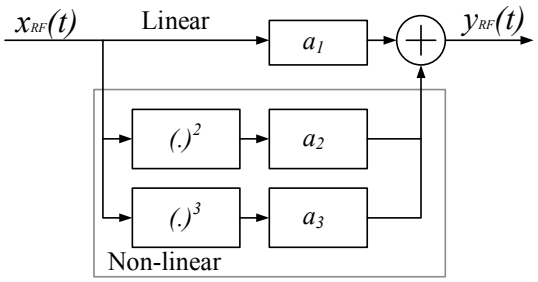

Fig. 3. A reduced non-linear model of LNA in multi-channel DRF-RXs.

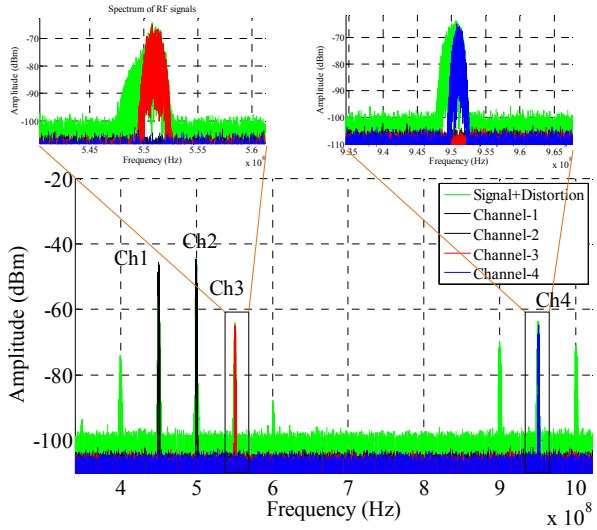

Fig. 4. LNA distortion in DRF-FX with 4 QPSK channels (f_1 = 450 MHz, f_2 = 500 MHz, f_3 = 550 MHz, and f_4 = 950 MHz).

As illustrated in Fig. 2, when the input signal has two frequency components (f_1, f_2), the output signal will have two harmonic groups: $n \times f_1$, $m \times f_2$, and inter-modulation $n \times f_1 \pm m \times f_2$. The distortion happens as soon as those components appear near the received signal frequency. For example, components $(2f_1 - f_2)$ and $(2f_2 - f_1)$ could distort f_1 and f_2. The other harmonics and inter-modulation, on the other hand, could distort other high-frequency signals.

A DRF-RX configuration with four QPSK signal channels was set up to confirm the models in (1)–(5) (Ch1 f_1 = 450 MHz, Ch2 f_2 = 500 MHz, Ch3 f_3 = 550 MHz, and Ch4 f_4 = 950 MHz). Fig.4 shows spectra of the signals including linear component and nonlinear distortions according to the models in (1)–(5) from the Matlab model. From the figure, intermodulation and harmonic distortions generated from Ch1 and Ch2 visibly influence the nearby Ch3 and far-away Ch4, respectively. In such situations, the SNR of Ch3 and Ch4 were severely degraded and this essentially requires techniques for the distortion compensations.

III. LNA Distortion Compensation Multichannel DRF-RXs using Adaptive LMS Algorithm

A. Structure of DRF-RXs With Reference Receiver

As analyzed in Part II, due to LNA's nonlinearity, large power signals will create distortion components, which distort themselves and other miniature channels. Therefore, distortion generated by high energy channels needs to be removed.

In this section, the distortion compensation scheme for DRF-RX is described in detail. The structure of the proposed RX comprises the main receiver and a reference receiver as depicted in Fig. 5. Only the former needs an LNA due to the requirements for the sensitivity. The latter does not have the LNA so that the received signal remains linear. The received signals from the main receiver are linearized by the distortions compensation circuits before passing to the demodulation. This structure is similar to the design approach in [9] However, the core algorithm was adapted accordingly to fit the distortion models for DRF-RXs, presented in Section II.

During the distortion removal process, the useful signal can be recovered by either subtracting or inverting the distortion components [9]. In this work, we focused only on the inversion technique. The underlying idea is to invert all LNA nonlinear effects by an adaptive compensation circuit. The structure of the circuit using this technique is shown in Fig. 6. The sampled signal from the main receiver $y_{RF}[n]$ is fed directly to the nonlinear compensation circuit while the sampled reference signal $y_{REF}(n)$ is passed to the LMS circuit to adjust the coefficients w(n). The final output $\hat{x}_{RF}[n]$ is expected to have only the linear components. This process is mathematically explained in the followings.

Let's denote $g_i(x[n])$ is the i-th order of the main receiver input $y_{RF}[n]$, thus

$$g_i(y_{RF}[n]) = y_{RF}^i[n], \text{ i} = 1,2,\ldots\text{k} \quad (6)$$

The current output of the compensation circuit expressed as

$$\hat{x}_{RF}[n] = \sum_{i=1}^{k} (\hat{w}_i) g_i(y_{RF}[n]) \quad (7)$$

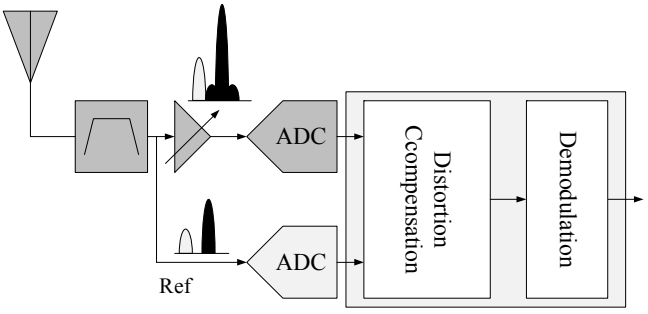

Fig. 5. Structure of the DRF-RXs with using reference receiver and distortion compensation circuit.

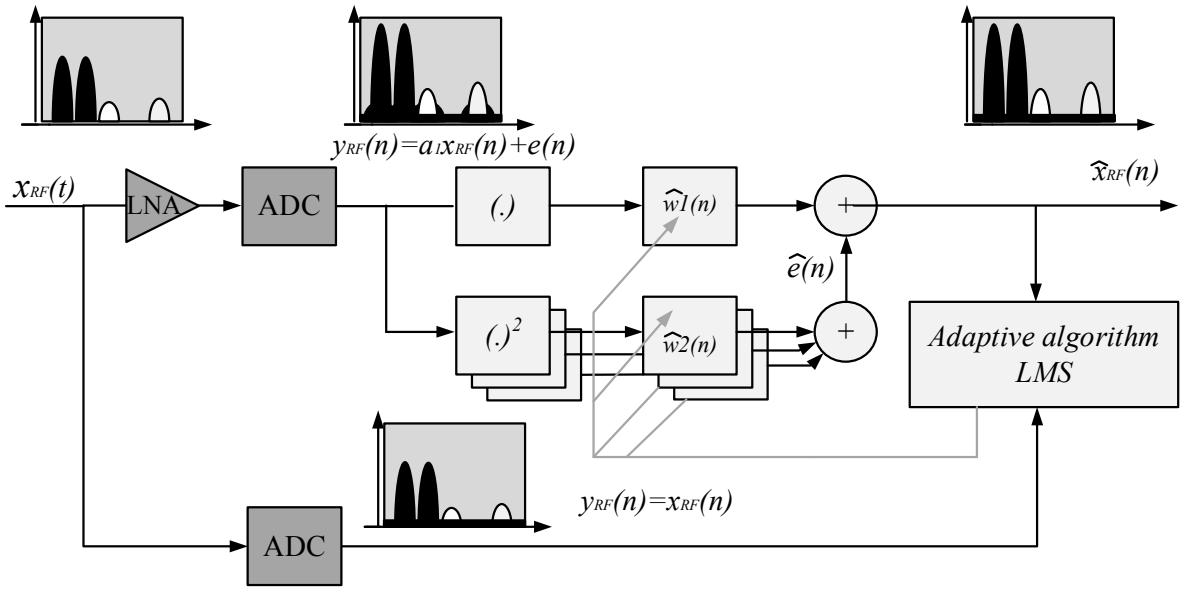

Fig. 6. The detailed structure of the distortion compensation circuit using the adaptive distortion inversion technique in DRF-RXs.

This output is fed back to the LMS block, where it is subtracted from the reference input $y_{REF}(n)$ for calculating the error

$$\hat{\varepsilon}[n] = y_{REF}(n) - \sum_{i=1}^{k} \widehat{w}_i g_i(y_{RF}[n]) \quad (8)$$

The LMS principally operates to minimize the square error $\hat{\varepsilon}[n]^2$ in (8). This process is done by taking the feedback error to dynamically adjust the nonlinear coefficient $\widehat{w}_i[n]$ as follows

$$\widehat{w}_i[n] = \widehat{w}_i[n-1] + \mu_i f_i(y_{RF}[n])\hat{\varepsilon}[n] \quad (9)$$

This process continues until all coefficients $\widehat{w}_i[n]$ stabilize at a fixed value, at that time the square error reaches the minimum [1]. During that process, $\hat{x}_{RF}[n]$ is asymptotically approaching the linear reference input $y_{REF}(n)$. After the LMS has been converged, the generated output $\hat{x}_{RF}[n] \approx y_{REF}(n)$. Thus, the transfer function of the compensation circuit at the LMS convergence is the inverse of the LNA's transfer function. As a result, all distortion impacts caused by LNA are rolled back at this stage. In other words, this helps to compensate all non-linear components caused by LNA while keeping the signal level adequate for further processing at the digital domain.

[1] This minimum is not necessary to be zero, for example, if there is a small DC bias component between $\hat{x}_{RF}[n]$ and $y_{REF}(n)$, this minimum can be a non-zero value. More details about LMS can be found in [18].

IV. Evaluation of The Distortion Compensation Schemes On Multichannel DRF-RX

To evaluate the distortion reduction effect of the proposed distortion inversion scheme described in the previous Sections, we implemented in Matlab the DRF-RXs model operating at the frequency band UHF (300MHz-1GHz). To suit the sampling frequency for the UHF band, a pair of high-speed ADCs, assumably capable of 4Gsps, are employed to directly digitalize the RF signal of the main and reference channels. (see Fig. 5).

We simulated four QPSK channels with each channel data rate is 4 Mbps. Among them, one channel is outside the receiver range and the other three are within the receiver band. The parameters of the channels are given as in Table I. This configuration is set up following some practical applications for mobile communication systems [21] and high-speed applications such as video transmission.

TABLE I. CONFIGURATION OF 4 SIMULATED QPSK CHANNELS IN THE IMPLEMENTED DRF-RX.

	Type	Symbol rate/Power	RF Carry Frequencies
Channel_1	QPSK	4 Mbps	$f_{RF1} = 450$ MHz
Channel_2	QPSK	4 Mbps	$f_{RF2} = 500$ MHz
Channel_3	QPSK	4 Mbps	$f_{RF3} = 550$ MHz
Channel_4	QPSK	4 Mbps	$f_{RF4} = 950$ MHz

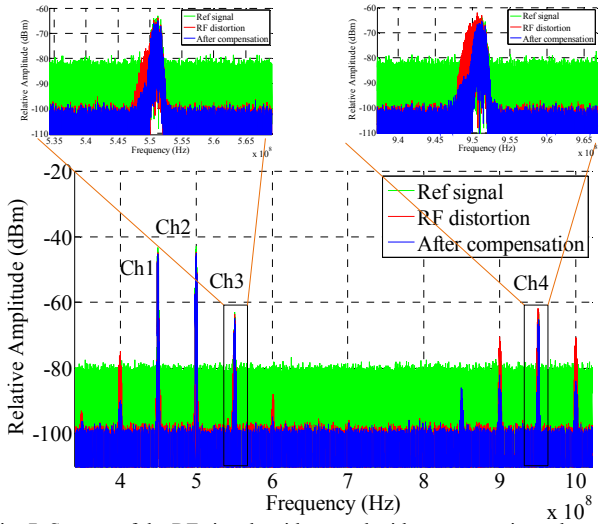

Fig. 7. Spectra of the RF signals without and with compensation schemes.

Two channels causing distortion are QPSK signals with carrier frequencies $f_1 = 450\ MHz$ (Ch1) and $f_2 = 500\ MHz$ (Ch2). The third and fourth channel are QPSK signals with carrier frequencies of $f_3 = 550$ MHz (Ch3) and $f_4 = 950$ MHz (Ch4).

From the analysis in [3, 12, 14, 19] the fourth and higher distortion orders have little impact on the LNA output and can be removed to reduce the complexity and area/energy cost of the compensation circuit. We did verify by the measurement using a commercial LNA (MAR 8ASM+ [17]) that with the -10 dBm input signal, the output of LNA would produce 2-order distortion at -40 dB, third-order distortion at -60 dB while the higher-order distortions are not observable. Therefore, to evaluate the proposed method, schemes in Section III are implemented with only up-to-third order distortion model.

The spectra of the LNA output signal before and after the distortion processing are shown in Fig. 8. Ch3 is intentionally set to be close to the distortion source (Ch1 and Ch2), so that it is affected by the third-order distortion components as in (5). In contrast, Ch4, locating far from the distortion sources, is affected by the even-order distortion components in (4).

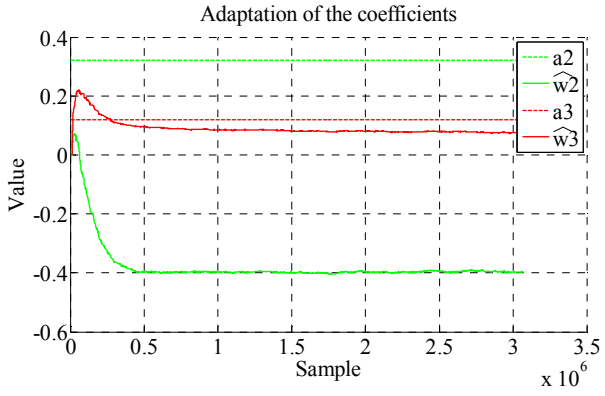

Fig. 8. The convergence of the nonlinear coefficients in (13) of the LMS circuit.

From the spectra figure, Ch3 distortion and the Ch4 distortion components have been visibly reduced after applying the proposed scheme. Specifically, the distortion compensation circuit helps to reduce the power level of the distortion components by ~15 dB for the Ch3 and ~25 dB for the Ch4 as compared to the power level when no compensation is applied.

Regarding the convergence speed of the LMS algorithm, Fig. 8 plots the parameters of the LMS circuits. The value of μ is chosen between [0.0001÷0.1] to balance the speed of convergence and the accuracy of the algorithm, the bigger the μ, the faster the convergence time but the larger the error. In this figure, a_i is the actual coefficients of the input signal before LNA, and $\widehat{w}_i$ is the dynamic LMS output coefficients to the compensation circuit. As can be seen from the figure, the conversion speed of these coefficients is reasonably good. Both the second and the third-order coefficients are converged after ~10^6 samples, which is just about a few milliseconds for a system clock of ~1 Ghz. These results confirm that the LMS algorithm would track well the changes in the inputs and can be suited for real-time processing.

Finally, we conduct a study on the performance of the receiver based on the BER. Here BER is calculated for Ch3 and Ch4, which are distorted by Ch1 and Ch2. Fig. 9(a)-(b) plot the BERs, statistically calculated from 10^6 QPSK samples for Ch3 and Ch4, respectively. BERs were calculated

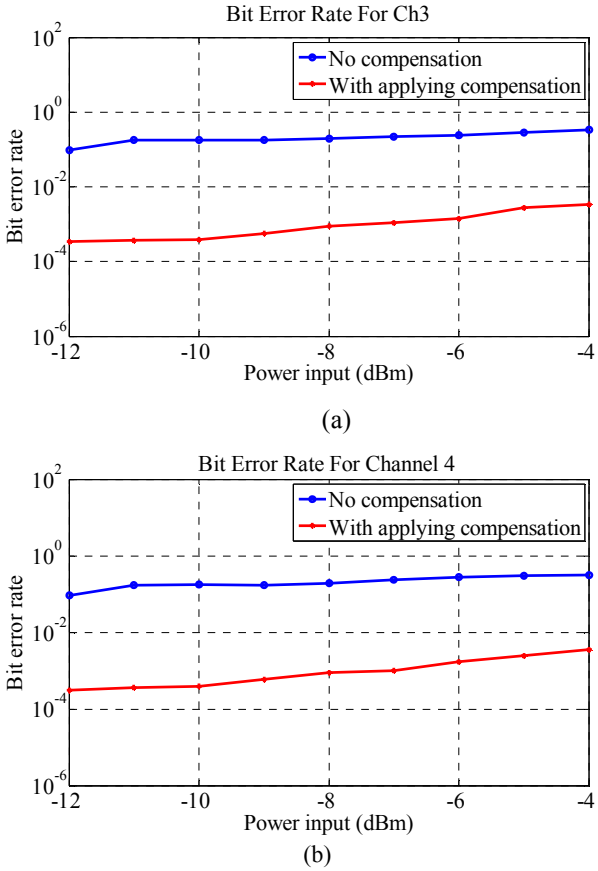

Fig. 9. BER of (a) Channel 3 and (b) Channel 4 in the case without and with compensation.

for the receiver with and without the compensation circuit with respect to the power level of the aggressor channels (i.e., Ch1 and Ch2).

It can be observed that BER clearly increases when there is an increase in the power level of the aggressor channels. Despite the difference in the nature of the distortion components (i.e., Ch3 (Ch4) is affected by the third (second) order distortion), the calculated BERs in both cases follow the same trend and are quite similar. Particularly, the receiver without the compensation severely affected by the distortion with very high BER (> 0.1), that would not satisfy the typical performance requirement even for audio communication [20]. By applying the compensation circuit, there is a significant BER improvement by 2 orders of the magnitude for both Ch3 and Ch4. Specifically, from Fig. 9, BER of ~10-3 can be achieved when the total power level of the RF signals are as high as -4 dBm.

V. CONCLUSIONS

In this work, we have systematically studied the impact of LNA nonlinearity on multichannel DRF-RXs. Based on the LNA's nonlinear model, we have proposed a distortion inversion circuit using a reference channel and an adaptive LMS algorithm. The circuit could adaptively and blindly compensate all types of distortion components regardless of the received frequency and/or the nature of the distortion sources. The effectiveness of the compensation technique has been demonstrated and quantified through a case study of 4 QPSK channels UHF direct RF digitization receivers. The simulation results show that the interested signals are successfully recovered and a great reduction in measured BER as compared to the non-distortion compensation receiver. Also, the distortion compensation using the inversion technique is straightforward to be implemented with an adequate convergence speed and hence is suited for a wide range of real-world applications.

ACKNOWLEDGEMENT

This research is funded by Vietnam National Foundation for Science and Technology Development (NAFOSTED) under grant number 102.01-2018.310

REFERENCES

[1] Software Defined Radio, Spectrum Analyzer, and Panoramic Adapter/ Available: http://www.rfspace.com/RFSPACE/SDR-IQ.html. [Accessed May 20, 2019].

[2] Perseus SDR - Software Defined 10 kHz - 30 MHz Receiver. Available: http://microtelecom.it/perseus/. [Accessed May 20, 2019].

[3] O. Jamin, *Broadband Direct RF Digitization Receivers*, Analog Circuits and Signal Processing 121, DOI 10.1007/978-3-319-01150-9_2, Springer International Publishing Switzerland 2014

[4] A. A. Abidi, "Direct-conversion radio transceivers for digital communications," *IEEE J. Solid-State Circuits*, vol. 30, no. 12, pp. 1399–1410, Dec. 1995.

[5] O. Jamin, V. Rambeau, F. Goussin, and G. Lebailly, "An rf frontend for multi-channel direct rf sampling cable receivers," *in Proc. ESSCIRC,*. Sep. 2011, pp. 347–350.

[6] B. Razavi, "Design considerations for direct-conversion receivers," *IEEE Trans. Circuits Syst. II, Analog Digit. Signal Process.*, vol. 44, no. 6, pp. 428–435, Jun. 1997.

[7] L. Anttila, M. Valkama, and M. Renfors, "Circularity-based I/Q imbalance compensation in wideband direct-conversion receivers," *IEEE Trans. Veh. Technol.*, vol. 57, no. 4, pp. 2099–2113, Jul. 2008.

[8] R. Vansebrouck, O. Jamin, P. Desgreys, and V.-T. Nguyen, "Digital distortion compensation for wideband direct digitization RF receiver," *in Proc. IEEE 13th Int. New Circuits Syst. Conf. (NEWCAS),* Jun. 2015, pp. 1–4.

[9] Jaakko Marttila, Markus Allénand Marko Kosunen, "Reference Receiver Enhanced Digital Linearization of Wideband Direct-Conversion Receivers" *IEEE Transactions On Microwave Theory And Techniques*, vol.65, no. 2, pp. 607-620, February 2017.

[10] Raphaël Vansebrouck, Chadi Jabbour, Olivier Jamin, and Patricia Desgreys, "Fully-Digital Blind Compensation of Non-Linear Distortions in Wideband Receivers" *IEEE Transactions on circuits And Systems-I: Regular Papers*, vol. 64, no. 8, pp. 2112-2123, August 2017.

[11] M. Grimm, M. Allen, J. Marttila, M. Valkama, and R. Thoma, "Joint mitigation of nonlinear rf and baseband distortions in wideband direct-conversion receivers," *Microwave Theory and Techniques, IEEE Transactions on*, vol. 62, no. 1, pp. 166–182, Jan 2014.

[12] Gharaibeh, Khaled M, *Nonlinear distortion in wireless systems: modeling and simulation with MATLAB*, John Wiley & Sons Ltd, 2012.

[13] Texas Instruments. "ADC32RF83 Dual-Channel, 14-Bit, 3-GSPS, RF Sampling Wideband Receiver, and Feed," ADC32RF83 datasheet Available: http://www.ti.com/product/ADC32RF83.

[14] Doug Stuetzle, "Understanding IP2 and IP3 Issues in Direct Conversion Receivers for WCDMA Wide Area Basestations*", Linear Technology.*

[15] M. R. Karim & M. Sarraf, "W-CDMA and cdma 2000" for 3G Mobile Network", McGraw-Hill Telecom. Professionals pp. 332-334, 2002.

[16] Texas Instruments. "ADC32RF45 Dual-Channel, 14-Bit, 3-GSPS RF-Sampling Analog-to-Digital Converter (ADC)," ADC32RF45 datasheet, Available: http://www.ti.com/product/ADC32RF45.

[17] MAR-8ASM+. http://www.minicircuits.com

[18] S. Haykin, *Adaptive Filter Theory*, 4th ed. Upper Saddle River, NJ, USA: Prentice-Hall, 2002.

[19] Admoon Andrawes "Multi-tone Analysis in Nonlinear Systems," 2nd International Conference on Advances in Computational Tools for Engineering Applications (ACTE), pp. 96-100, 2012.

[20] Jean Walrand, Pravin Varaiya, "High-Performance Communication Networks" (Second Edition), 2000.

[21] Aselsan. "PRC V/UHF SDR Handheld Radios." Available: https://www.aselsan.com.tr/en-us/capabilities/military-communication-systems/v-uhf-military-radios/prc-v-uhf-sdr-handheld-radios.